DALTON
FULL PAPER

Synthesis, structure and characterisation of $Ln_5O(OPr^i)_{13}$ with Ln = Nd, Gd or Er

Mikael Kritikos,[a] Marat Moustiakimov,[a] Maria Wijk[b] and Gunnar Westin *[b]

[a] *Department of Structural Chemistry, Arrhenius Laboratory, Stockholm University, SE - 106 91 Stockholm, Sweden*
[b] *Department of Inorganic Chemistry, Ångström Laboratory, Uppsala University, SE - 751 21 Uppsala, Sweden. E-mail: Gunnar.Westin@mkem.uu.se*

Received 27th March 2001, Accepted 3rd May 2001
First published as an Advance Article on the web 18th June 2001

The molecular and basically isostructural oxo-alkoxides $Ln_5O(OPr^i)_{13}$ (Pr^i = 2-propyl) with Ln = Nd (**1**) and Gd (**2**) were synthesized by metathesis of $LnCl_3$ and $KOPr^i$, in combination with stoichiometric hydrolysis, in 2-propanol-containing solvents. $Er_5O(OPr^i)_{13}$ **3** was obtained as co-product to an erbium aluminium 2-propoxide with an Er : Al ratio of *ca.* 3 : 1, from the reaction of $15KOPr^i + H_2O + Al(OPr^i)_3$ with $5ErCl_3$, in toluene–2-propanol. The solid state structures of **1**–**3** were obtained by single-crystal X-ray diffraction. The characterisations were made with differential scanning calorimetric measurements, UV-Vis and FT-IR spectroscopy. The molecule contains an M_5O fragment with the configuration of a square pyramid and the oxo-oxygen atom slightly above the basal plane. FT-IR measurements showed that the molecular structure of the alkoxide was retained, to a large extent, when dissolved in toluene–2-propanol (2 : 1) or hexane. Investigations by UV-Vis and FT-IR spectroscopy showed that $Ln_5O(OPr^i)_{13}$ reacted with $Al_4(OPr^i)_{12}$ (Ln : Al = 1 : 3) in toluene–2-propanol to form $LnAl_3(OPr^i)_{12}$ within 2 hours at 80 °C.

1.0 Introduction

Alkoxides are important precursors in the preparation of advanced ceramic materials by the organic sol–gel route.[1,2] The reactions taking place in the sol–gel process are quite complicated, but a good knowledge about the precursors and the intermediates in solution gives increased possibilities of tailoring the properties of the ceramic product. An area that has received considerable interest in recent times is the sol–gel processing of rare-earth metal ion containing glasses as bulk and wave-guide materials.[3] Such additions yield glasses that can be used for lasers operating in the near-IR region or for frequency up-conversion devices converting near-IR light into visible light.

Neodymium, gadolinium and erbium 2-propoxides have been prepared both by metathesis of $LnCl_3$ and $NaOPr^i$ and by dissolution of the elemental lanthanide. Misra *et al.* reported the formation of $Ln(OPr^i)_3$ from $3NaOPr^i$ and $LnCl_3{\cdot}3HOPr^i$ including Ln = Nd, Gd or Er, in refluxing-2-propanol.[4,5] The data given for the alkoxides of Nd and Gd were not possible to use for comparison with our materials, and the data on the erbium compound did not give a good match with any of the characterised erbium oxo- or non-oxo-2-propoxides that we have prepared.[6] Anderson *et al.* used similar metathesis conditions but obtained blue crystals, determined by single-crystal X-ray diffraction to be $Nd_6Cl(OPr^i)_{17}$.[7] Brown and Mazdiyasni also obtained 2-propoxides, assumed to be $Ln(OPr^i)_3$, by dissolution of the corresponding metals in refluxing 2-propanol containing solvents.[8] The spectroscopic data given for these materials are consistent with those for $Ln_5O(OPr^i)_{13}$ prepared by us, showing that the compounds are the same. Later studies by Helgesson *et al.* on neodymium 2-propoxides prepared from the metal in a very similar way as by Mazdiyasni *et al.* showed that most of the material formed consisted of solvated tetramers, $Nd_4(OPr^i)_{12}(HOPr^i)_4$, while a part of it consisted of the oxo-2-propoxide, $Nd_5O(OPr^i)_{13}(HOPr^i)_2$.[9,10] The structure of the latter compound was determined by single-crystal X-ray techniques to have a trigonal bipyramidal arrangement of the metal atoms around the central oxo-oxygen. Other rare-earth (Yb[11] and Er[6]), yttrium-[12] and indium-[11] oxo-2-propoxides structurally determined have the formula $M_5O(OPr^i)_{13}$, with a square pyramidal arrangement of the metal atoms around the oxo-oxygen lying in the basal plane. An FT-IR study of the entire series of lanthanide 2-propoxides (except for Pm) showed that it was possible to prepare the square pyramidal $Ln_5O(OPr^i)_{13}$ molecule for all Ln^{3+}, but solvated oxo-2-propoxides formed more easily with Ce and La.[13]

In this work we report the structural characterisation by single-crystal X-ray diffraction of the basically isostructural $Ln_5O(OPr^i)_{13}$, with Ln = Nd, Gd or Er, crystallised in the monoclinic crystal system. The alkoxides of Nd and Gd were prepared by a new synthesis route, namely combined metathesis and hydrolysis, and structurally determined for the first time. $Er_5O(OPr^i)_{13}$ has structurally been described before, but as crystallising in an orthorhombic space group.[6] The $Er_5O(OPr^i)_{13}$ molecules, having very weak interactions with their neighbours, are virtually identical in the two types of packing, *i.e.* in the monoclinic and orthorhombic structures, which makes it possible to analyse the sensitivity of different parts of the molecule to packing effects. The new crystal packing structure was obtained when $Er_5O(OPr^i)_{13}$ formed as a co-product in the search for new 2-propoxides of Er and Al in the Er-rich part of the Er–Al–(oxo)-2-propoxide system. The $Nd_5O(OPr^i)_{13}$ compound, consisting of the square pyramidal molecules found in most other lanthanide oxo-2-propoxides, is new and differs from the expected trigonal bipyramidal $Nd_5O(OPr^i)_{13}(HOPr^i)_2$ obtained by other researchers by metal dissolution in 2-propanol-containing solvents and crystallisation at low temperature. The compounds are characterised by their FT-IR and UV-Vis spectra, differential scanning calorimetry curves, melting points and solubility, and by the feasibility of reaction with $Al_4(OPr^i)_{12}$ to form $LnAl_3(OPr^i)_{12}$, which has attracted much attention in recent years.

2.0 Experimental

2.1 Equipment and chemicals

A scanning electron microscope (SEM, JEOL 820) equipped for energy dispersive analysis of X-ray spectra (energy disper-

DOI: 10.1039/b102798k

sive spectroscopy, EDS; LINK AN 10000) was used for determining elemental contents (Nd, Gd, Er, K and Cl) of hydrolysed and dried samples. The detection limit of these elements is normally *ca.* 0.3 atom%. FT-IR spectra were recorded from 5000 to 360 cm^{-1}, with a Bruker IFS-55 spectrometer. The solid samples were investigated as KBr tablets, and the dissolved samples in a 0.1 mm path length KBr cell. The homogeneity and identity of the contents obtained by the syntheses were investigated by a large number of IR and SEM-EDS analyses on small crystals or clusters of crystals and on larger areas of bulk samples. In this case the IR studies were normally performed on paraffin mulls between KBr plates. UV-Visible spectra were recorded in the range 200–900 nm with a Perkin-Elmer Lambda 19 or a Philips PU 8740 spectrometer, from solutions in sealed quartz cuvettes using a slit of 0.3 nm or smaller. The behaviour on heating was studied in the range 40–260 °C, at a heating rate of 5 °C min^{-1}, with a differential scanning calorimeter (Perkin-Elmer DSC-2), using air-tight steel compartments. Crystals were observed during heating in sealed glass capillaries, using a solid-block melting-point apparatus.

The toluene, hexane and 2-propanol used were dried by distillation over CaH_2. The anhydrous $LnCl_3$ (Ln = Nd, Gd or Er of 99.9% grade, Strem) were used as purchased, and the $Al_4(OPr^i)_{12}$ (Aldrich) was recrystallised before use. All preparations were performed in a glove-box (Mecaplex GB80) containing dry, oxygen-free argon.

2.2 Synthesis of $Ln_5O(OPr^i)_{13}$

$Nd_5O(OPr^i)_{13}$ 1 and $Gd_5O(OPr^i)_{13}$ 2. 12.79 mmol (0.500 g) K was dissolved in 20 ml of a 1 : 1 (vol : vol) toluene–2-propanol mixture, followed by addition of 0.85 ml 1 M water in the same solvent. One hour later, 4.263 mmol of $LnCl_3$ were added, and after 48 hours at room temperature the mixture was centrifuged to sediment the KCl formed in the reaction. On evaporation of the solution part a mass was obtained consisting almost exclusively of $Ln_5O(OPr^i)_{13}$. After dissolution in hexane and centrifugation a very small amount of solid material was precipitated and evaporation of the solvent part yielded highly pure and crystalline $Ln_5O(OPr^i)_{13}$ in 90–95% yields. SEM-EDS analyses showed no contamination by K and Cl. The IR and UV-Vis spectra of these compounds are shown in Figs. 1, 2 and 4, respectively. For the neodymium alkoxide the $NdCl_3$ source was found important; while the reaction proceeded at room temperature with the source given above, no reaction occurred even after two weeks at 75 °C with another source.

$Er_5O(OPr^i)_{13}$ 3. 25.58 mmol (1.000 g) K were dissolved in 20 ml of a 1 : 1 (vol : vol) toluene–2-propanol mixture, followed by addition of 1.70 ml 1 M water in the same solvent. Then, 1.71 mmol $Al(OPr^i)_3$ (0.348 g) and 8.526 mmol (2.333 g) $ErCl_3$ were added, and after 48 hours at room temperature the mixture was centrifuged to sediment the precipitated KCl. On slow evaporation of the pink solution part a crystal mixture of an erbium aluminium alkoxide with an approximate Er : Al ratio of 3 : 1 and $Er_5O(OPr^i)_{13}$ were obtained. SEM-EDS analyses showed no contamination by K and Cl.

Compounds **1**–**3** are very soluble in toluene and hexane, but only sparingly soluble in 2-propanol.

2.3 Crystallography

Irregularly shaped crystals of **1**, **2** and **3** were glued by a thin layer of paraffin inside a glass capillary that was melt-sealed in a glove-box. For all three compounds X-ray diffraction data were collected employing a Stoe four-circle diffractometer, using monochromatised Mo-Kα radiation and the ω–2θ scan technique. Data for **1**, **2** and **3** were corrected for background, Lorentz, polarisation and absorption effects. Numerical absorption correction was performed with the program package X-SHAPE.[14,15]

The structures were solved by direct methods and refined using the programs SHELXS 86[16] and SHELXL 97,[17] respectively. The metal and oxygen atoms were refined anisotropically for **1**, **2** and **3**. The isopropyl groups were treated slightly different in the three compounds. For **1**, in the isopropyl groups connected to O(1), O(2), O(3), O(4), O(7) the central carbon was refined anisotropically. The terminal carbons were refined isotropically and disordered over two sites with a common atomic displacement parameter and the sum of the occupancy factors fixed to 1.0. The rest of the isopropyl groups were refined in a similar fashion, except that in this case all carbons were isotropic and disordered. The restraints on the isopropyl groups were introduced as follows: all O–C bond distances were restrained to the same refined value of 1.386(5) Å and the C–C distances to 1.469(5) Å. The non-bonding 1,3 O···C distances were restrained to 2.364(8) Å and the C···C distances to 2.506(8) Å. For **2**, all the carbon atoms were refined isotropically. All bonding 1,2 O–C distances were restrained to the expected value of 1.42 Å, and the C–C distances to 1.52 Å. Anti bumping restraints of 2.5 Å were also applied to the following non-bonding 1,3 C···C distances: C(24)···C(25), C(34)···C(35), C(36)···C(37), C(38)···C(39). The anisotropic displacement parameters of the O(2) and O(3) oxygen atoms were restrained by ISOR.[17] For **3**, the central carbon atoms of the isopropyl groups were refined anisotropically and the rest of the atoms isotropically. All bonding O–C distances were restrained to the expected value of 1.42 Å, C–C distances to 1.52 Å. Anti bumping restraints of 2.5 Å were also applied to the following non-bonding 1,3 C···C distances: C(22)···C(23), C(24)···C(25), C(34)···C(35). The anisotropic displacement parameters of O(8) and all central carbon atoms of the isopropyl groups were restrained by ISOR.[17] For **1**, **2** and **3** all H atoms were placed in calculated positions, with isotropic displacement parameters 1.2 times the U_{iso} of their respective parent C atom. CH_3 (C–H 0.98 Å) and CH (C–H 1.00 Å) groups were constrained to idealised geometry, with H atoms riding. Further crystallographic details for **1**, **2** and **3** are summarised in Table 1.

CCDC reference numbers 158362–158364.

See http://www.rsc.org/suppdata/dt/b1/b102798k/ for crystallographic data in CIF or other electronic format.

3.0 Results and discussion

3.1 Synthesis

By metathesis of $NdCl_3$ or $GdCl_3$ and $KOPr^i$ without hydrolysis, as well as by dissolution of the lanthanide metals in toluene–2-propanol solvents, we obtained almost exclusively 2-propoxides other than $Ln_5O(OPr^i)_{13}$, while combined metathesis and stoichiometric hydrolysis exclusively yielded $Ln_5O(OPr^i)_{13}$. It was expected that metathesis without hydrolysis or metal dissolution of the metals in 2-propanol containing solvents should yield $Ln_5O(OPr^i)_{13}$, but we found that a stoichiometric amount of water is needed for the synthesis of the oxo-alkoxide. The combined metathesis and hydrolysis has also been used for the high yield synthesis of $Er_5O(OPr^i)_{13}$, but in that case the crystal obtained was orthorhombic.[6]

The $Er_5O(OPr^i)_{13}$ was found as a co-product in the investigation of the Er–Al–OPr^i system where $Er_2Al_2(OPr^i)_{12}(HOPr^i)_2$[18] and $ErAl_3(OPr^i)_{12}$[19] have structurally been characterised before. In this system yet another hetero bimetallic alkoxide exists with an approximate Er : Al ratio of 3 : 1, which unfortunately has eluded several attempts of structural determination by the single crystal X-ray technique. This hetero bimetallic alkoxide is the most Er-rich one in the Er–Al–(oxo)-2-propoxide system, and when higher Er : Al ratios are used in the metathesis the

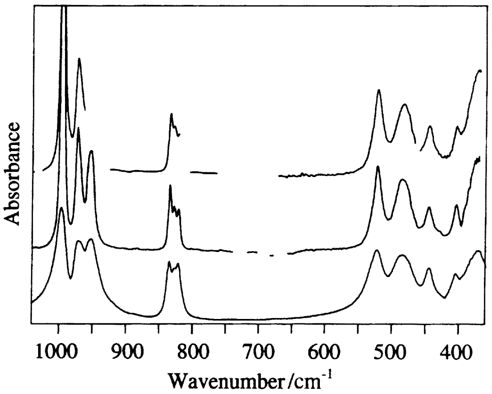

Fig. 1 FT-IR spectrum of $Nd_5O(OPr^i)_{13}$ as a solid in KBr (lower curve), hexane solution (middle curve) and toluene–2-propanol (2 : 1) solution (upper curve). The spectrum has been removed where the solvent background absorptions were too strong to be subtracted properly.

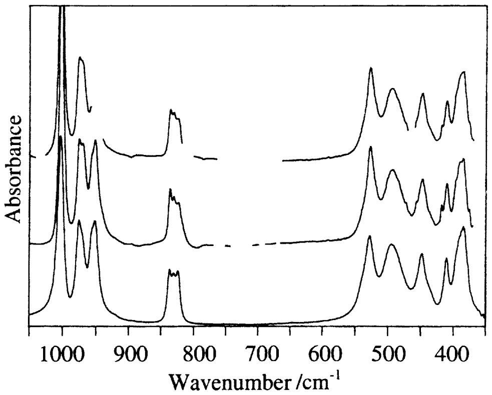

Fig. 2 FT-IR spectra of $Gd_5O(OPr^i)_{13}$. Details as in Fig. 1.

excess of Er is found as $Er_5O(OPr^i)_{13}$. The structure determination of such a crystal showed it to be monoclinic.

Comparison of the IR and UV-Vis data given by Mazdiyasni *et al.* on alkoxides obtained by metal dissolution in 2-propanol containing solvents, formulated as $Ln(OPr^i)_3$, showed similarities great enough for us to believe that these compounds are the same as our compounds formed with stoichiometric hydrolysis and structurally determined as $Ln_5O(OPr^i)_{13}$.

Two pure 2-propoxides have earlier been characterised structurally as products after dissolution of neodymium metal in toluene–2-propanol: $Nd_4(OPr^i)_{12}(HOPr^i)_4$ and $Nd_5O(OPr^i)_{13}(HOPr^i)_2$.[9] The latter has the same ratio of Nd to oxo-oxygen as $Nd_5O(OPr^i)_{13}$, but contains two additional and easily lost $HOPr^i$ adducts. In our studies, $Nd_5O(OPr^i)_{13}$ was found as a very minor product when dissolving neodymium metal in toluene–2-propanol, while metathesis combined with hydrolysis even in pure 2-propanol yielded only $Nd_5O(OPr^i)_{13}$. The difference in oxo-alkoxide products probably lies in the crystallisation process: Helgesson *et al.* made the crystallisation at −20 °C and mounted the crystals at approximately −80 °C, whereas we have made both the crystallisation and mounting of the crystals at room temperature. Thus, it seems that the solvated oxo-2-propoxide is not stable at room temperature.

3.2 Characterisation and properties of $Ln_5O(OPr^i)_{13}$

Spectroscopic characterisation of $Nd_5O(OPr^i)_{13}$. An FT-IR spectrum (KBr) of solid $Nd_5O(OPr^i)_{13}$, in the range 1050–360 cm^{-1}, is shown in Fig. 1. The bands below 600 cm^{-1} are assigned as due to Nd–O vibrations, while the bands in the region 1250–800 cm^{-1} are assigned as due to C–O, C–C vibrations. Peaks in this region were found at: 1161, 1149sh, 1130, 1124, 1117sh, 997, 973, 969sh, 956sh, 953, 835, 828, 822, 538sh, 523, 486, 476sh, 445, 430sh, 405, 380sh, 371 cm^{-1}. The FT-IR spectra of $Nd_5O(OPr^i)_{13}$ dissolved in toluene–2-propanol (2 : 1) and hexane show a very good resemblance to that of solid $Nd_5O(OPr^i)_{13}$, as seen in Fig. 1. This indicates that the molecular structure is retained on dissolution.

The UV-Vis spectra of $Nd_5O(OPr^i)_{13}$ in toluene–2-propanol solvents in the range 190–900 nm showed bands typical of Nd^{3+}.[20] The fine structures of the absorption peaks of lanthanide alkoxides have been shown to be useful in identifying different homo- and hetero-bimetallic alkoxides, but this is the first time a neodymium alkoxide has been studied in this way.[6,21] Most strong peaks of the Nd^{3+} ions were found to be sensitive to the coordination sphere, but the peaks assigned as due to the $^4G_{5/2},^2G_{7/2} \longleftarrow {}^4I_{9/2}$ (550–630 nm) and the $^4D_{1/2},{}^4D_{3/2},{}^4D_{5/2} \longleftarrow {}^4I_{9/2}$ (340–380 nm) transitions were chosen for identification, due to their high sensitivity and strength. The fine structures of these absorptions of **1** in toluene and toluene–2-propanol (1 : 9) solution are shown in Fig. 4. It can be observed that there are no changes of the spectrum from the pure toluene to the toluene–2-propanol (1 : 9) solvent composition, which indicates that no solvated structure such as $Nd_5O(OPr^i)_{13}(HOPr^i)_2$ is obtained, even in the presence of high concentrations of 2-propanol.

Spectroscopic characterisation of $Gd_5O(OPr^i)_{13}$. An FT-IR spectrum of solid **2**, in the range 1050–360 cm^{-1}, is shown in Fig. 2. Peaks in the Gd–O and C–O, C–C vibration region were found at: 1166, 1132, 1124, 1004, 976, 971sh, 956sh, 952, 837, 831, 824, 538sh, 528, 495, 448, 437sh, 410, 385 cm^{-1}. The FT-IR spectra of **2** dissolved in toluene–2-propanol (2 : 1) and hexane closely resemble that of the solid, which indicates that, as with the corresponding compounds of Nd and Er, the solid-state structure is retained both in polar and non-polar solvents.

Unfortunately, due to the f^7 electronic configuration, the absorptions of Gd^{3+} ions are quite weak and found only in the UV region, where they are obscured by absorptions of most solvents, such as 2-propanol.

Spectroscopic characterisation of $Er_5O(OPr^i)_{13}$. No difference in the IR spectrum of the solid state $Er_5O(OPr^i)_{13}$ was observed between the alkoxide prepared in this work and that obtained by combined metathesis and hydrolysis, reported earlier.[6] This is to be expected, since the molecules are very similar in the two types of packing, and interactions between the molecules are weak; therefore crystallographic site symmetry splitting is not expected. Also, we are not certain that the entire samples consist of only one crystalline phase, but an investigation of this has not been pressed since it is of little interest for the alkoxide as a precursor to ceramic materials or as a catalyst in organic synthesis. After dissolution, the molecules ought to be identical and thus the solution state UV-Vis and FT-IR spectroscopic studies given before should apply.

Thermal properties of $Ln_5O(OPr^i)_{13}$. Visual studies of $Ln_5O(OPr^i)_{13}$ (Ln = Nd or Gd) crystals during heating in melt-sealed glass capillaries showed no changes up to *ca.* 250 °C, where the materials became more opaque and the neodymium compound acquired a lighter blue colour. The DSC curves of $Ln_5O(OPr^i)_{13}$, shown in Fig. 3, show endotherms with onsets at Nd 167 °C and Gd 168 °C, and minima at Nd 176 °C and Gd 171 °C. The peaks corresponded to energies of Nd *ca.* 14 kJ mol^{-1} and Gd *ca.* 5 kJ mol^{-1}. However, the difference in energies is very small and might be within the experimental error. Although no melting was visually observed, the endothermic peaks of the two compounds are believed to stem from melting and not from decomposition, since the endotherms could be reproduced after cooling. The same features have been found in the DSC run of $Er_5O(OPr^i)_{13}$.[6]

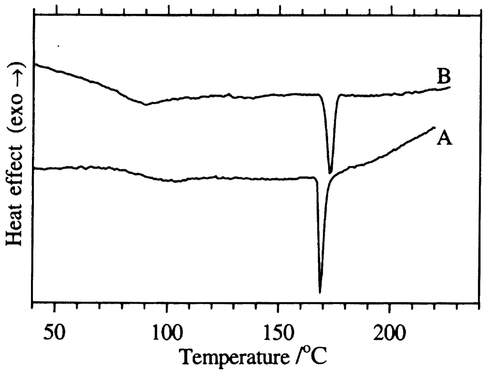

Fig. 3 DSC curves of $Nd_5O(OPr^i)_{13}$ (A) and $Gd_5O(OPr^i)_{13}$ (B) obtained in an inert atmosphere.

Reactivity of $Ln_5O(OPr^i)_{13}$ with $Al_4(OPr^i)_{12}$. The $Y_5O(OPr^i)_{13}$ and $Nd_5O(OPr^i)_{13}(HOPr^i)_2$ molecules have been reported to be very stable towards reaction with $Al_4(OPr^i)_{12}$, in the case of the yttrium compound even under reflux.[6,11,12] We have previously studied the reaction of $Y_5O(OPr^i)_{13}$ and $Er_5O(OPr^i)_{13}$ with $Al_4(OPr^i)_{12}$ in toluene–2-propanol and found that the reactivity is rather high, being complete after 2 h at 75 °C.[6] This reaction is of interest not only for the understanding of basic alkoxide chemistry, but also from the practical use in the preparation of a suitable precursor for the preparation of Ln-doped wave guides. In this case it is of importance to avoid formation of Ln-rich clusters within the wave guide, since such clustering severely reduces the optical properties by non-radiative quenching. Hence, a hetero bimetallic precursor containing Ln^{3+} ions surrounded by three $Al(OPr^i)_4^-$ tetrahedra would be much better than a mixture of the $Ln_5O(OPr^i)_{13}$ cluster and $Al_4(OPr^i)_{12}$, normally used in the metal–organic sol–gel preparation of glassy Ln–Al–Si–O wave guides. Glassy Er–Al–(Ti)–Si–O wave guides prepared with $ErAl_3(OPr^i)_{12}$ as precursor have also shown that unusually high erbium contents can be incorporated before the non-radiative losses reduce the NIR fluorescence and frequency up-conversion.[22–24] In this connection it might be of interest to investigate the reactivity also of the two larger and more basic Gd^{3+} and Nd^{3+} ions in order to see if notable changes in reactivity are present.

According to the UV-Vis studies of a toluene–2-propanol (2 : 1) solution of **1** and $Al_4(OPr^i)_{12}$ in the ratio Nd : Al = 1 : 3 the reaction was quite slow at room temperature. Heating to 80 °C speeded up the reaction greatly, and the formation of $NdAl_3(OPr^i)_{12}$ was complete after 2 h (see Fig. 4). IR studies of the material obtained by evaporation of the solution after 2 h at 80 °C showed peaks of $NdAl_3(OPr^i)_{12}$ only (see Fig. 5).

Since peaks in the UV-visible region were only found below 280 nm for Gd^{3+}, studies on systems containing 2-propanol, which is strongly absorbing below *ca.* 300 nm, could not be done. Evaporation of a solution of **2** and $Al_4(OPr^i)_{12}$, prepared with a Gd : Al ratio of 1 : 3 yielded after 2 hours at 80 °C only $GdAl_3(OPr^i)_{12}$. The identity of $GdAl_3(OPr^i)_{12}$ was obtained by its homogeneous 1 : 3 Gd to Al composition in SEM-EDS and by comparison of its IR spectrum with that of the X-ray determined $ErAl_3(OPr^i)_{12}$ and the starting compound $Al_4(OPr^i)_{12}$ (see Fig. 5).

Thus, the reactivity of $Nd_5O(OPr^i)_{13}$ and $Gd_5O(OPr^i)_{13}$ is similar to those of the yttrium and erbium congeners, and it is possible to prepare the isolated Ln^{3+} precursor, $LnAl_3(OPr^i)_{12}$ with Ln = Gd and Nd, from $Al_4(OPr^i)_{12}$ and $Ln_5O(OPr^i)_{13}$ by just heating the solution for a limited time.

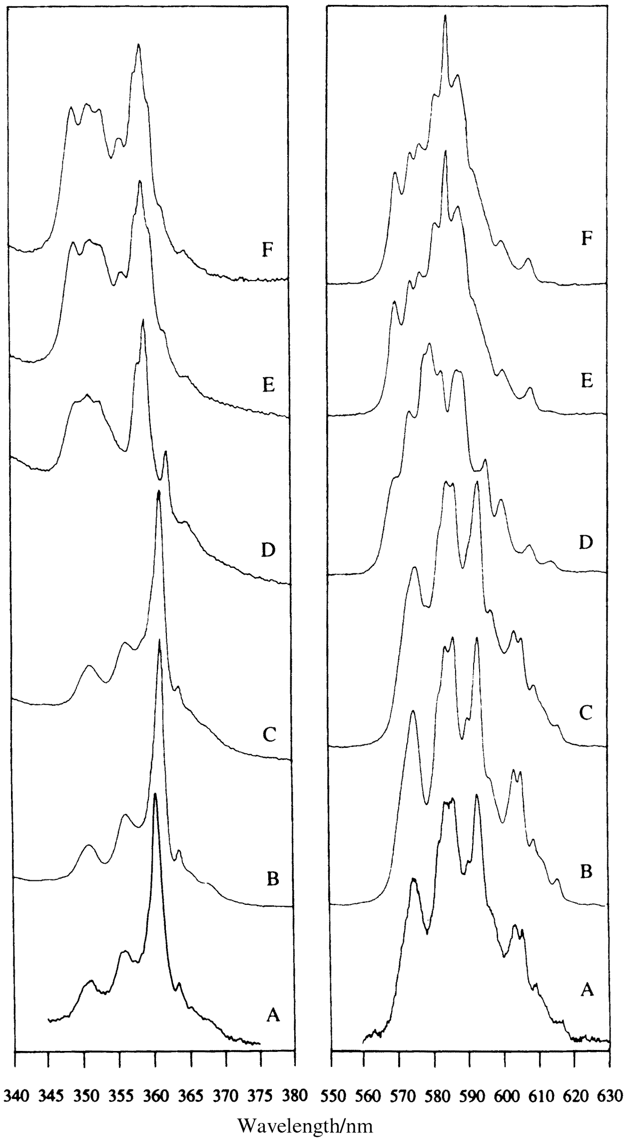

Fig. 4 Absorption spectra showing the $^4D_{1/2},^4D_{3/2},^4D_{5/2} \longleftarrow {}^4I_{9/2}$ (340–380 nm) and $^4G_{5/2},^2G_{7/2} \longleftarrow {}^4I_{9/2}$ (550–630 nm) Nd^{3+} transitions of $Nd_5O(OPr^i)_{13}$ dissolved in toluene–2-propanol (1 : 9) (A) and toluene (B), $Nd_5O(OPr^i)_{13}$ and $Al_4(OPr^i)_{12}$ with an Nd to Al ratio of 1 : 3 after 12 h at room temperature (C), 1.25 h at 80 °C (D), 2 h at 80 °C (E) and $NdAl_3(OPr^i)_{12}$ in toluene–2-propanol (F).

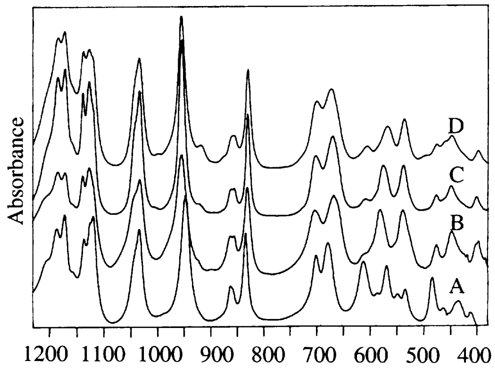

Fig. 5 FT-IR spectrum of: $Al_4(OPr^i)_{12}$ (A), $ErAl_3(OPr^i)_{12}$ (B), $Gd_5O(OPr^i)_{13}$ + $Al_4(OPr^i)_{12}$ after 2 h at 80 °C (C), $Nd_5O(OPr^i)_{13}$ + $Al_4(OPr^i)_{12}$ after 2 h at 80 °C (D).

3.2 Structural features

Molecular structure of $Ln_5O(OPr^i)_{13}$. The obtained molecular structures are shown in Fig. 6, together with the atom labelling scheme used for the metal and oxygen atoms. The bond-distance distribution and calculated bond valence sums (bvs values) indicate that the lanthanide atoms are all trivalent. Each molecule consists of five lanthanide atoms, one oxo-oxygen

Table 1 Selected crystal data for $Nd_5O(OPr^i)_{13}$ **1**, $Gd_5O(OPr^i)_{13}$ **2** and $Er_5O(OPr^i)_{13}$ **3**

	1	2	3
Empirical formula	$C_{39}H_{91}Nd_5O_{14}$	$C_{39}H_{91}Gd_5O_{14}$	$C_{39}H_{91}Er_5O_{14}$
Formula weight	1505.05	1570.55	1620.42
Crystal system	Monoclinic	Monoclinic	Monoclinic
Space group	$P2_1/n$ (no. 14)	$P2_1/n$ (no. 14)	$P2_1/n$ (no. 14)
a/Å	12.912(5)	12.7837(16)	12.769(4)
b/Å	21.611(12)	21.248(7)	21.432(19)
c/Å	21.722(6)	21.552(6)	21.297(5)
β/°	91.54(3)	91.085(16)	91.27(2)
V/Å^3	6059(4)	5853(4)	5827(6)
Z	4	4	4
T/K	220(1)	150(1)	170(1)
μ(Mo-Kα)/mm^{-1}	4.26	5.64	7.17
N(meas.), N(ind.), R(int)	10279, 8362, 0.0397	6702, 5487, 0.0363	6023, 3913, 0.0740
N(obs.), N(par.)	4490, 470	3372, 328	3913, 394
$R1$, $wR2$ ($I > 2\sigma(I)$)	0.0518, 0.1326	0.0589, 0.1688	0.0791, 0.2246

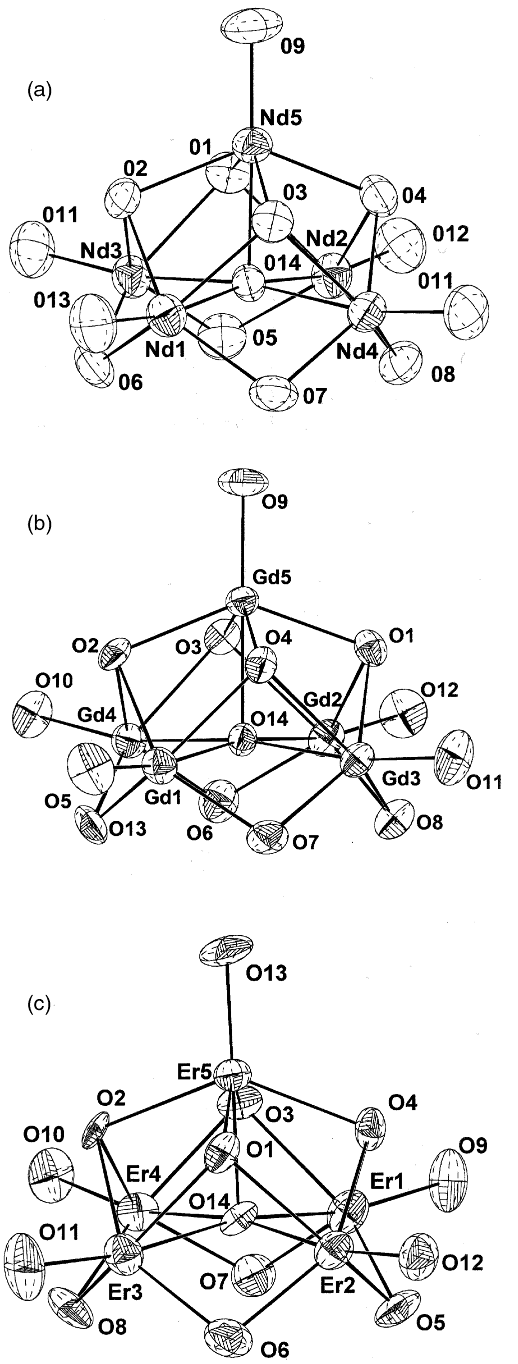

Fig. 6 ORTEP[25] view of the metal oxygen framework of **1** (a), **2** (b) and **3** (c) showing 30% probability displacement ellipsoids.

Table 2 Selected interatomic distances (Å) for $Nd_5O(OPr^i)_{13}$

Terminal M–O		μ_5 M–O	
Nd(1)–O(13)	2.123(11)	Nd(1)–O(14)	2.448(8)
Nd(2)–O(12)	2.084(11)	Nd(2)–O(14)	2.499(8)
Nd(3)–O(10)	2.085(11)	Nd(3)–O(14)	2.479(8)
Nd(4)–O(11)	2.082(11)	Nd(4)–O(14)	2.502(8)
Nd(5)–O(9)	2.084(10)	Nd(5)–O(14)	2.440(8)
μ M–O		M–M	
Nd(1)–O(6)	2.345(11)	Nd(1)–Nd(3)	3.497(2)
Nd(1)–O(7)	2.322(11)	Nd(1)–Nd(4)	3.498(2)
Nd(2)–O(5)	2.320(11)	Nd(1)–Nd(5)	3.635(2)
Nd(2)–O(8)	2.324(11)	Nd(2)–Nd(3)	3.497(2)
Nd(3)–O(5)	2.334(9)	Nd(2)–Nd(4)	3.496(2)
Nd(3)–O(6)	2.304(12)	Nd(2)–Nd(5)	3.636(2)
Nd(4)–O(7)	2.333(11)	Nd(3)–Nd(5)	3.631(2)
Nd(4)–O(8)	2.323(10)	Nd(4)–Nd(5)	3.634(2)
μ_3 M–O		μ_3 M–O	
Nd(1)–O(2)	2.523(10)	Nd(4)–O(3)	2.526(9)
Nd(1)–O(3)	2.517(9)	Nd(4)–O(4)	2.496(10)
Nd(2)–O(1)	2.535(10)	Nd(5)–O(1)	2.427(9)
Nd(2)–O(4)	2.528(9)	Nd(5)–O(2)	2.424(10)
Nd(3)–O(1)	2.507(10)	Nd(5)–O(3)	2.423(10)
Nd(3)–O(2)	2.531(9)	Nd(5)–O(4)	2.414(9)

and 13 2-propoxo groups. This gives the molecular formula $Ln_5O(OPr^i)_{13}$ and, indicating the coordination around the oxygen atoms, the molecular formula becomes $Ln_5(\mu_5\text{-}O)(\mu_3\text{-}OPr^i)_4(\mu\text{-}OPr^i)_4(OPr^i)_5$.

The Ln atoms are all coordinated to the oxo-oxygen and to five 2-propoxo groups, which gives a distorted octahedral configuration around each lanthanide atom. From the data in Tables 2, 3 and 4 it is seen that the Ln–O distances differ depending on the size of the metal atoms and the coordination around the oxygen atom involved. The Ln–μ_5-O distances within one Ln_5O unit differ only slightly for $Nd_5O(OPr^i)_{13}$ and $Gd_5O(OPr^i)_{13}$, whereas they span a broader range in $Er_5O(OPr^i)_{13}$. The apical Ln atoms have the shortest Ln–μ_5-O distances. The Ln–μ_3-O distances depend on whether or not the Ln atom in question is apical or basal, the first one being shorter. The μ-O atoms bridging between basal lanthanide atoms have rather equal distances for **1**, **2** and **3**, respectively. The terminal Ln–O bonds are the shortest and these also have the largest M–O–C angles, ranging between 165 and 177°, in comparison with the M–O–C angles for μ-O and μ_3-O, which are in the range 125–138 and 120–130°, respectively. The short distances and very obtuse angles could indicate some interaction between the ligands and the s,p orbitals of the Nd^{3+} ions, forming multiple bonds between Nd and O. The trends seen in the compounds **1**, **2** and **3** for Ln–O bond lengths and Ln–O–C bond angles are also found for other $M_5O(OPr^i)_{13}$ (M = In, Yb, Er or Y[6,11,12]).

Table 3 Selected interatomic distances (Å) for Gd$_5$O(OPr^i)$_{13}$

Terminal M–O		μ_5 M–O	
Gd(1)–O(13)	2.084(19)	Gd(1)–O(14)	2.391(12)
Gd(2)–O(12)	2.114(16)	Gd(2)–O(14)	2.398(13)
Gd(3)–O(11)	2.060(12)	Gd(3)–O(14)	2.418(9)
Gd(4)–O(10)	2.080(10)	Gd(4)–O(14)	2.412(10)
Gd(5)–O(9)	2.048(13)	Gd(5)–O(14)	2.387(11)
μ M–O		M–M	
Gd(1)–O(5)	2.283(16)	Gd(1)–Gd(3)	3.3865(16)
Gd(1)–O(7)	2.261(11)	Gd(1)–Gd(4)	3.3908(19)
Gd(2)–O(6)	2.261(15)	Gd(1)–Gd(5)	3.5279(15)
Gd(2)–O(8)	2.247(12)	Gd(2)–Gd(3)	3.390(2)
Gd(3)–O(7)	2.234(13)	Gd(2)–Gd(4)	3.3891(16)
Gd(3)–O(8)	2.32(2)	Gd(2)–Gd(5)	3.527(2)
Gd(4)–O(5)	2.269(13)	Gd(3)–Gd(5)	3.5225(12)
Gd(4)–O(6)	2.238(19)	Gd(4)–Gd(5)	3.5248(17)
μ_3 M–O		μ_3 M–O	
Gd(1)–O(2)	2.473(10)	Gd(4)–O(2)	2.473(15)
Gd(1)–O(4)	2.488(12)	Gd(4)–O(3)	2.435(11)
Gd(2)–O(1)	2.466(14)	Gd(5)–O(1)	2.352(11)
Gd(2)–O(3)	2.477(11)	Gd(5)–O(2)	2.362(11)
Gd(3)–O(1)	2.481(11)	Gd(5)–O(3)	2.320(15)
Gd(3)–O(4)	2.490(15)	Gd(5)–O(4)	2.346(14)

Table 4 Selected interatomic distances (Å) for Er$_5$O(OPr^i)$_{13}$

Terminal M–O		μ_5 M–O	
Er(1)–O(9)	2.04(3)	Er(1)–O(14)	2.29(2)
Er(2)–O(12)	2.04(3)	Er(2)–O(14)	2.33(2)
Er(3)–O(11)	2.04(3)	Er(3)–O(14)	2.38(2)
Er(4)–O(10)	2.06(3)	Er(4)–O(14)	2.39(2)
Er(5)–O(13)	2.00(3)	Er(5)–O(14)	2.30(2)
μ M–O		M–M	
Er(1)–O(5)	2.24(3)	Er(1)–Er(2)	3.301(3)
Er(1)–O(7)	2.16(3)	Er(1)–Er(4)	3.299(4)
Er(2)–O(5)	2.24(3)	Er(1)–Er(5)	3.428(3)
Er(2)–O(6)	2.20(3)	Er(2)–Er(3)	3.303(4)
Er(3)–O(6)	2.23(3)	Er(2)–Er(5)	3.425(3)
Er(3)–O(8)	2.23(3)	Er(3)–Er(4)	3.303(3)
Er(4)–O(7)	2.29(3)	Er(3)–Er(5)	3.438(4)
Er(4)–O(8)	2.26(3)	Er(4)–Er(5)	3.426(3)
μ_3 M–O		μ_3 M–O	
Er(1)–O(3)	2.43(2)	Er(4)–O(2)	2.45(2)
Er(1)–O(4)	2.38(3)	Er(4)–O(3)	2.34(3)
Er(2)–O(1)	2.43(2)	Er(5)–O(1)	2.30(3)
Er(2)–O(4)	2.36(2)	Er(5)–O(2)	2.33(2)
Er(3)–O(1)	2.40(3)	Er(5)–O(3)	2.29(2)
Er(3)–O(2)	2.36(2)	Er(5)–O(4)	2.32(2)

In all of the square pyramidal M$_5$O alkoxide structures determined hitherto the oxo-oxygen atoms lie above the basal plane.[6,11,12] In the case of **1**, **2**, and **3** the displacement from the basal plane is 0.211(7), 0.20(1) and 0.22(2) Å, respectively. This displacement is comparable to those in *o*-Y$_5$O(OPr^i)$_{13}$ (0.20 Å),[12] *m*-Yb$_5$O(OPr^i)$_{13}$ (0.19 Å),[11] *m*-In$_5$O(OPr^i)$_{13}$ (0.16 Å)[12] and *o*-Er$_5$O(OPr^i)$_{13}$ (0.16 Å).[6]

Comparison of orthorhombic and monoclinic Er$_5$O(OPr^i)$_{13}$. Comparing the molecular structure of orthorhombic and monoclinic Ln$_5$O(OPr^i)$_{13}$ shows that the main difference, although very small, is in the oxygen atom displacement from the basal plane; 0.211(7) Å in the present monoclinic structure compared to 0.162(2) Å in the orthorhombic structure. The molecules in both orthorhombic and monoclinic Er$_5$O(OPr^i)$_{13}$ phases form close packings of the . . . ABAB . . . type (Fig. 7). In both polymorphs the distance between the molecules is approximately 12 Å. However, the orientation of the molecules in the layers is significantly different in the two phases as can be seen from Fig. 8a and 8b. In the layers depicted one can denote the molecules with the apical metal atom pointing approximately up with '+' and those with the apical atom pointing down with '−'. The '+' and '−' in the layers of both phases alternate, but there is no way to superimpose them.

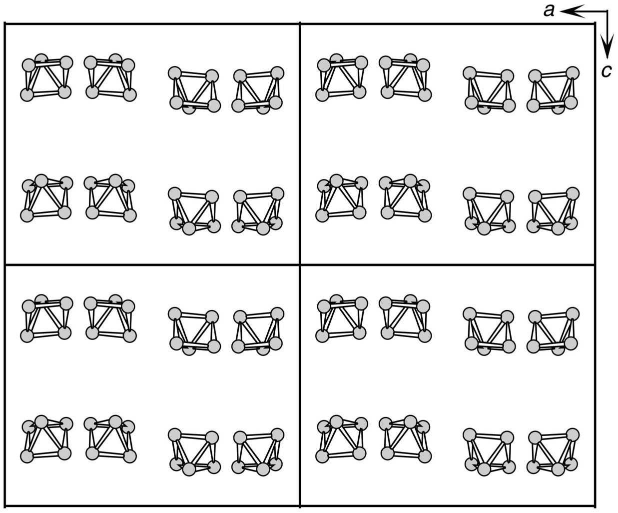

Fig. 7 The (AB) layer of molecules of the orthorhombic Er$_5$O(OPr^i)$_{13}$. Only the metal core is shown.

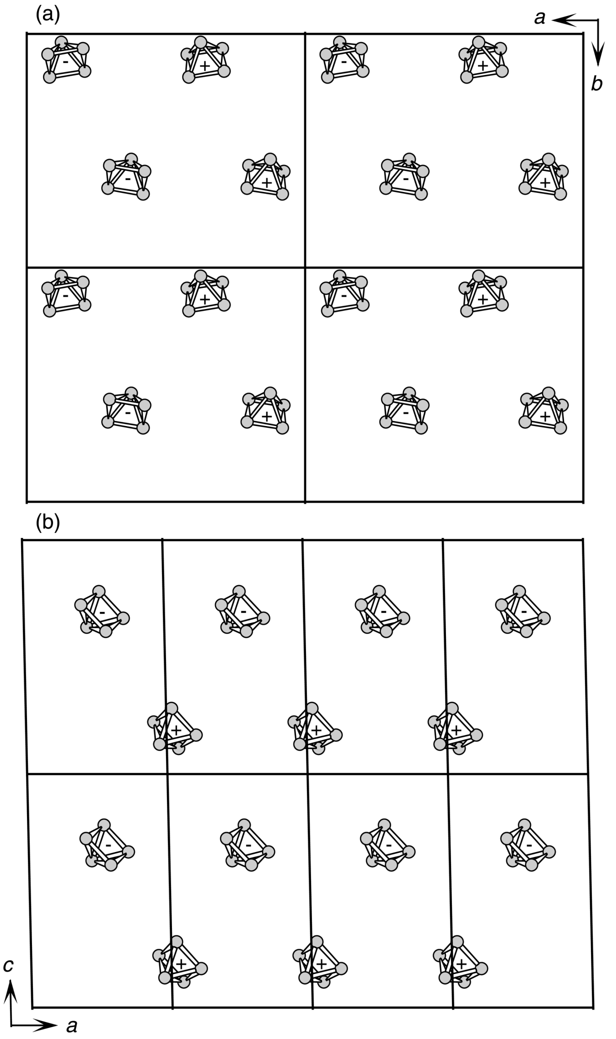

Fig. 8 The layer of molecules of orthorhombic Er$_5$O(OPr^i)$_{13}$ (a) and monoclinic Er$_5$O(OPr^i)$_{13}$ (b). Only the metal core is shown.

Comparison of Nd$_5$O(OPr^i)$_{13}$ with Nd$_5$O(OPr^i)$_{13}$(HOPr^i)$_2$. It is interesting that two alternative structures can be obtained

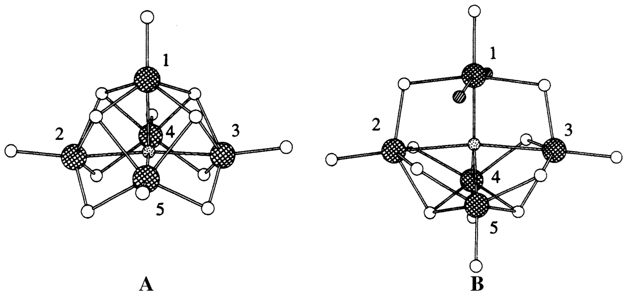

Fig. 9 The molecular structures of $Nd_5O(OPr^i)_{13}$ (A) and $Nd_5O(OPr^i)_{13}(HOPr^i)_2$ (B). The Nd atoms appear as large, cross-hatched circles; the oxo-oxygens small, spotted circles; and the H-donor oxygens small, striped circles. (The crystallographic data of $Nd_5O(OPr^i)_{13}(HOPr^i)_2$[9] are taken from ref. 32.)

with the same ratio of Nd to oxo-oxygen. We believe, as mentioned above, that the solvated structure is obtained at low temperatures only, since we were not able to prepare it even from pure 2-propanol at room temperature. The Nd–O cores of the two oxo-alkoxides are shown in Fig. 9. The structural differences are small, and the coordination around the Nd atoms is retained as distorted octahedral. Only four bonds need to be broken and four to be formed, of which two are to the apical Nd(1) atom from the added solvating 2-propanols for a transformation to $Nd_5O(OPr^i)_{13}(HOPr^i)_2$. The number of alkoxo-bridges between the apical Nd(1) atom and the basal Nd(2–5) atoms is reduced to a large extent, while it is increased between the basal Nd(2–5) atoms. The Nd(1)–O_{oxo} bond length is shortened from 2.53 to 2.42 Å, and the Nd(2–5)–O_{oxo} bonds are divided into two groups: one with long bonds (2.72 Å) and one with short (2.46 Å). The Nd–μ_5-O_{oxo} oxygen bond lengths in the $Nd_5O(OPr^i)_{13}(HOPr^i)_2$ molecule are in the order expected for steric reasons in a trigonal bipyramid, *i.e.* there are 3 short bonds (2.36–2.46 Å) in the horizontal plane of the bipyramid and two long bonds (2.72 Å) along the vertical axis.

The molecular structure obtained by addition of two 2-propanol adducts is very similar to that of $Ln_4TiO(OPr^i)_{14}$ ($Ln = Sm$[26] or $(Tb_{0.9}Er_{0.1})$[27]). In these molecules the apical position with the solvated Nd atom is exchanged for a Ti atom bonded in the same manner with two μ-OPr^i bridges and one short bond to the oxo-oxygen. The compound is not solvated, and the Ti atom is five-coordinated with two bonds pointing in peripheral directions, instead of the two solvate $HOPr^i$ groups and the terminal 2-propoxo group of Nd(1). Thus, it seems that addition of H, as solvating 2-propanol groups, changes the charge balance of the molecule to resemble that obtained with a tetravalent Ti atom. This phenomenon seems to be rather general for both homo- and hetero-metallic alkoxides. For example, in the series $M_{6+x}Sb_4O_4(OEt)_{16}(HOEt)_{4-2x}$ (M = Mn or Ni; $x = 0$, 1 or 2) the total number of positive charges in the rather similar molecules is kept constant by exchanging 2 H^+ for one M^{2+} on solvation in ethanol-rich solvents.[28,29] There are also examples where a metal ion is completely replaced by H^+ in the position of the missing metal ion. One such molecule is $Er_2Zr_2O(OPr^i)_{12}(HOPr^i)_3$, which has approximately the same trigonal bipyramidal structure as that found for $Nd_5O(OPr^i)_{13}(HOPr^i)_2$, if the three protons of the solvating $HOPr^i$ groups located around the position where Nd(1) would be situated are taken into account.[30] This is also the case for $Ce_4O(OPr^i)_{10}(HOPr^i)$.[31]

4.0 Conclusion

Three basically isostructural alkoxides of the formula $Ln_5O(OPr^i)_{13}$ ($Ln = Nd$, Gd or Er) have been synthesized and structurally determined by single-crystal X-ray techniques. $Ln_5O(OPr^i)_{13}$ ($Ln = Nd$ or Gd) were prepared in high yields by the new route: combined metathesis and stoichiometric hydrolysis. The addition of water was found necessary to obtain high yields of $Ln_5O(OPr^i)_{13}$, which contradicts some earlier reports that $Ln_5O(OPr^i)_{13}$ alkoxides of Ln^{3+} or In^{3+} were obtained without water addition; in some cases exceptional precautions against moisture were taken.[10–12] Only in the case of dissolution of metallic Nd has the non-oxo alkoxide been obtained together with the oxo-alkoxide.[9] $Er_5O(OPr^i)_{13}$ was obtained as a co-product in the synthesis of erbium aluminium 2-propoxides. $Nd_5O(OPr^i)_{13}$ is a new non-solvated variant of the earlier known $Nd_5O(OPr^i)_{13}(HOPr^i)_2$, and $Gd_5O(OPr^i)_{13}$ is here described for the first time. $Er_5O(OPr^i)_{13}$ has been described structurally before, but interestingly, in our case, has been obtained in a new monoclinic space group, although with very similar molecular units.

As the molecule contains five closely connected Ln atoms, and at room temperature is stable towards dissociation and reactions with alkoxides such as $Al_4(OPr^i)_{12}$, it is not suitable for sol–gel preparation of Ln-doped glassy laser amplifiers, since clustering of the Ln^{3+} ions reduces the optical yield severely. Heating an Ln : Al (1 : 3) mixture of $Ln_5O(OPr^i)_{13}$ and $Al_4(OPr^i)_{12}$ at 80 °C, however, yielded $LnAl_3(OPr^i)_{12}$, in which the Ln^{3+} ions are isolated from each other, and which is therefore a good precursor. This reactivity of $Ln_5O(OPr^i)_{13}$ also contradicts reports of this reaction with Ln = Y and Nd.[9,12]

Acknowledgements

The Swedish Natural Science Research Council (NFR) is acknowledged for financing this project. Dr K. Jansson is thanked for performing the DSC measurements. Dr M. Wijk wishes to thank the Royal Swedish Science Academy for financial support.

References

1 C. D. Chandler, C. Rogers and M. J. Hampden-Smith, *Chem. Rev.*, 1993, **93**, 1205.
2 G. W. Scherer and C. J. Brinker, *Sol-Gel Science*, Academic Press Ltd., London, 1990.
3 M. J. Weber, *J. Non-Cryst. Solids*, 1990, **123**, 208.
4 S. N. Misra, T. N. Misra, R. N. Kapoor and R. C. Mehrotra, *Chem. Ind.*, 1963, 120.
5 S. N. Misra, T. N. Misra and R. C. Mehrotra, *Aust. J. Chem.*, 1968, **21**, 797.
6 G. Westin, M. Kritikos and M. Wijk, *J. Solid State Chem.*, 1998, **141**, 168.
7 R. A. Andersen, D. H. Tempelton and A. Zalkin, *Inorg. Chem.*, 1978, **17**, 1962.
8 L. M. Brown and K. S. Mazdiyasni, *Inorg. Chem.*, 1970, **9**, 2783.
9 G. Helgesson, S. Jagner, O. Poncelet and L. Hubert Pfalzgraf, *Polyhedron*, 1991, **10**, 1559.
10 L. G. Hubert-Pfalzgraf, *New J. Chem.*, 1995, **19**, 727.
11 D. C. Bradley, H. Chudzynska, D. M. Frigo, M. E. Hammond, M. B. Hursthouse and M. A. Mazid, *Polyhedron*, 1990, **9**, 719.
12 O. Poncelet, W. J. Sartain, L. G. Hubert-Pfalzgraf, K. Folting and K. G. Caulton, *Inorg. Chem.*, 1989, **28**, 263.
13 G. Westin, M. Moustiakimov and M. Kritikos, unpublished work.
14 STOE X-RED, Data Reduction Program, Version 1.07/Windows, STOE & Cie, Darmstadt, 1996.
15 STOE X-SHAPE, Crystal Optimisation for Numerical Absorption Correction, Version 1.01/Windows, STOE & Cie, Darmstadt, 1996.
16 G. M. Sheldrick, SHELXS 86, Program for the Solution of Crystal Structures, University of Göttingen, 1986.
17 G. M. Sheldrick, SHELXL 97, Program for the Refinement of Crystal Structures, University of Göttingen, 1997.
18 M. Kritikos, M. Wijk and G. Westin, *Acta Crystallogr., Sect. C*, 1998, **54**, 576.
19 M. Wijk, R. Norrestam, M. Nygren and G. Westin, *Inorg. Chem.*, 1996, **35**, 1077.
20 K. B. Yatsimirskii and N. K. Davidenko, *Coord. Chem. Rev.*, 1979, **27**, 223.

21 G. Westin, R. Norrestam, M. Nygren and M. Wijk, *J. Solid State Chem.*, 1998, **135**, 149.

22 G. Westin, Å. Ekstrand, E. Zanghellini and L. Börjesson, *J. Phys. Chem. Solids*, 2000, **61**, 67.

23 G. Westin, M. Wijk, Å. Ekstrand, M. Kritikos and E. Wikstad, *Long Abstr.*, *Fifth Congress of the Am. I. Chem. Eng.*, Conference 96, San Diego, CA, 1996.

24 C. K. Ryu, H. Choi and K. Kim, *Appl. Phys. Lett.*, 1995, **66**, 2496.

25 C. K. Johnson, ORTEP II, Report ORNL-5138, Oak Ridge National Laboratory, Oak Ridge, TN, 1976.

26 S. Daniele, L. G. Hubert-Pfalzgraf, J. C. Daran and S. Halut, *Polyhedron*, 1994, **13**, 927.

27 M. Moustiakimov, M. Kritikos and G. Westin, *Acta Crystallogr., Sect. C*, 1998, **54**, 29.

28 G. Westin, *Chem. Commun.*, Stockholm University, 1994, **4**, 1.

29 G. Westin, *J. Sol-Gel Sci. Technol.*, 1998, **12**, 203.

30 G. Westin, M. Wijk, M. Moustiakimov and M. Kritikos, *J. Sol-Gel Sci. Technol.*, 1998, **13**, 125.

31 K. Yunlu, P. S. Gradeff, N. Edelstein, W. Kot, G. Shalimoff, W. E. Streib, B. A. Vaarstra and K. G. Caulton, *Inorg. Chem.*, 1991, **30**, 2317.

32 F. H. Allen and O. Kennard, *Chem. Des. Automat. News*, 1993, **8**, 1.